Kinetic Aspects of the Electrodissolution of Zinc in Bromate-Containing Alkaline Solutions

鋅在含溴酸鹽的鹼性溶液中的電化學溶解動力特性

doi:10.6967/JCICE.200605.0261

Journal of the Chinese Institute of Chemical Engineers, 37(3), 2006

中國化學工程學會會誌, 37(3), 2006

作者/Author： 張裕祺(Yu-Chi Chang);林岱儀(Dai-Yi Lin);林俊一(Chun-I Lin)

頁數/Page： 261-268

出版日期/Publication Date：2006/05

J. Chin. Inst. Chem. Engrs., Vol. 37, No. 3, 261-268, 2006

Kinetic Aspects of the Electrodissolution of Zinc in Bromate-Containing Alkaline Solutions

Yu-Chi Chang[1]
Department of Chemical and Materials Engineering, Tamkang University
Tamsui, Taipei Hsien 251, Taiwan

Dai-Yi Lin[2] **and Chun-I Lin**[3]
Department of Chemical Engineering, National Taiwan University of Science and Technology
Taipei 106, Taiwan

Abstract— The effect of bromate ions on the anodic behavior of zinc electrodes in potassium hydroxide solutions has been investigated experimentally using the rotating disk electrode technique. The total dissolution current was observed to decrease with the increasing concentration of the bromate ions. The experiments also showed that the potential required for the onset of passivation increased anodically with the addition of potassium bromate but rapidly reached a stable value that depended on the hydrodynamic condition. The Tafel slope became smaller with the introduction of potassium bromate. Based on the experimental results, a kinetic model describing the dissolution process was developed and tested. Good agreement between the experimental results and the model predictions supports our hypothesis that the reduction of bormate proceeds in parallel with the anodic dissolution of a zinc electrode in alkaline electrolyte solutions.

Key Words : Zinc, Bromate, KOH, Anodic dissolution, Kinetic model

INTRODUCTION

The electrochemical behavior of zinc in alkaline electrolyte solutions has been studied extensively due to its importance in battery uses (Binder, 1999; Littauer and Cooper, 1984; Pletcher and Walsh, 1993; Zhang, 1996). Many investigations have been conducted to determine the characteristics of this system (Armstrong and Bell, 1971; Aslam and Harrison, 1981; Bockris *et al.*, 1972; Chang and Prentice, 1989; Liu *et al.*, 1981; Popova, 1972; Prentice *et al.*, 1991). Although many researchers have studied the anodic behavior of zinc electrodes in pure alkaline electrolytes, few papers have examined the kinetic aspects of zinc dissolution processes in the presence of additives. Flerov (1959) investigated the effects of silicates and lithium compounds on the performance of zinc anodes in supersaturated zincate electrolytes. It was reported that the use of additives inhibited passivation of the zinc anode. Prostakov *et al.* (1961) examined the anodic behavior of zinc in alkaline solutions containing sodium chromate and potassium bromate, using a galvanostatic technique. They found that potassium bromate produced an increase in the current required for the onset of the passivation of zinc. Sato *et al.* (1971) studied the effects of carbonate on the anodic dissolution and the passivation of zinc electrodes in concentrated potassium hydroxide solutions. Accelerated passivation due to the presence of carbonate was reported. Marshall *et al.* (1977) also studied the effect of potassium silicate on the dissolution of zinc in alkali, but they found that the addition of silicate resulted in inhibition of zinc dissolution and favored passivation of the zinc anode. Kawamura and Maki (1980) observed that calcium hydroxide could effectively trap the discharge product of zinc electrodes when the concentration of potassium hydroxide was less than 3M. Cachet *et al.* (1981) found that the presence of NBu_4Br additives increased the cycle life of the zinc electrode. Morgan *et al.* (1981) reported that additives like chloride ions, silicate, phosphate, and polymaleic acid were not able to increase the passivation time of zinc in alkali dissolving under completely diffusion-dominated conditions. Sharma (1986, 1988a, 1988b) found the presence of calcium hydroxide improved the performance of the zinc electrode in Zn/aqueous KOH electrolyte/NiOOH cells.

The potential for raising the critical current density required for the onset of passivation of zinc electrodes in alkaline solutions through the addition of bromate makes the specific system technologi-

---

[1] 張裕祺, To whom all correspondence should be addressed
[2] 林岱儀
[3] 林俊一

cally very attractive. However, very little effort has been devoted to understanding the electrochemical characteristics of this system. Furthermore, no previous studies have modeled the kinetics of anodic dissolution of zinc in alkaline solutions containing bromate. In order to obtain a better understanding of the relevant electrode processes, we have conducted experiments using the rotating disk electrode technique in conjunction with slow potential sweep measurements. On the basis of the experimental results, a kinetic model was developed and tested in order to characterize the kinetic processes that occurred during the anodization of zinc electrodes in potassium hydroxide solutions containing bromate additives.

EXPERIMENTAL

A three-electrode, two-compartment electrolysis cell made of Teflon was used in all of the experiments. The solution volume of the sample compartment, 1.8 L, was sufficient to prevent any change in the potassium hydroxide concentration during anodic dissolution of zinc in an alkaline solution in each experimental run. A Pt foil was used as a counter electrode and was placed in the sample compartment. The potential of the zinc electrode was monitored through a Luggin capillary versus a mercury-mercuric oxide reference electrode placed in a potassium hydroxide solution with the same concentration as that in the sample compartment. The reference electrode was contained in a second compartment.

All electrolytic solutions were prepared from analytical grade chemicals and 10 megaohm-cm deionized water. No zincates were initially present in each experimental run. The solutions were sparged with high purity nitrogen prior to use, and a nitrogen blanket was maintained throughout the experiments. Prior to each run, the zinc electrode was cleaned by immersing it in dilute sulfuric acid, micropolished with 0.3 micron alumina, and rinsed in a stream of deionized water.

Rotating disk experiments were carried out on a Pine Instrument ASR rotator with a model AFDT 136 disk assembly and a RDE 3 potentiostat. Zinc disks, 0.5 cm in diameter and 99.99% pure, were used in all of the experiments. Current-potential traces were generated on a Hewlett-Packard model 7044A X-Y recorder. Temperature variation was controlled to within 0.1°C using a Thermomix 1480 thermostat.

Since our experimental setup did not include the self-compensating instruments, the experimental results obtained were subjected to ohmic potential drop correction following the tests. Of all the contributions to the ohmic resistance, usually, the ohmic potential drop between the reference electrode probe and the working electrode was the dominant one and could be approximately estimated experimentally and theoretically. For the classical case of a rotating disk electrode at constant potential in an insulating plane, it has been shown that (Nanis and Kesselman, 1971)

$$V(r = 0, z) = V_0\,(2/\pi)\,\tan^{-1}(a/z), \qquad (1)$$

where z is the distance in the normal direction from the disk, r is the radial coordinate, a is the disk radius, and $V_0 = V(r, z=0)$ is the potential at the disk surface. In addition, Newman (1966) proved that

$$V_0 = I / 4ka, \qquad (2)$$

where k is the conductivity of the electrolyte and I is the current passing through the electrolytic cell. Let V_{ohm} be the ohmic potential drop under consideration; then $V_{ohm}=V(r, z=0)–V(r=0, z)$. This is the expression used to correct the ohmic potential drop for the experimental data obtained. It should be noted that this expression is exact in primary current distribution situations.

RESULTS

Typical ohmic potential drop corrected polarization curves for the steady state slow potentiodynamic sweep response of polycrystalline zinc in potassium hydroxide solutions with and without bromate addition are illustrated in Fig. 1. Clearly, the shapes of the current-potential curves in the presence and absence of bromate look very much alike; however, zinc passivated at a slightly more anodic potential in the bromate-containing solution. This figure also shows that the total dissolution current was lowered by the addition of bromate in all of the regions: initial dissolution, active dissolution, prepassive, and passive. The decrease of the total current might have been due to the reduction of bromate, which will be explained in the next section.

To examine the behavior of the zinc electrode in bromate-containing solutions in detail, polarization measurements on the zinc rotating disk electrode in potassium hydroxide solutions with different potassium bromate concentrations were conducted. Typical results are shown in Fig. 2. This figure shows that the current required for the onset of passivation decreased significantly with the increasing content of potassium bromate. In Fig. 2(b), the cyclic voltammogram of a zinc electrode in a 1.0 M KOH + 0.1 M $KBrO_3$ solution shows one peak with the total current in the cathodic regime (the first peak) and another peak with the total current in the anodic regime (the second peak) during the anodic polarization sweep.

Figure 3 depicts the primary passive potentials

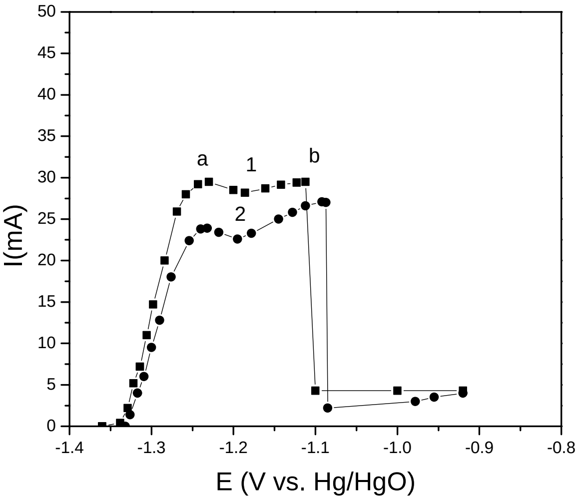

Fig. 1. Current-potential relationship on a rotating disk electrode: 2400 rpm, 2 mV/s, 29°C. Curve 1: 1.0 M KOH; curve 2: 1.0 M KOH+2 g/L $KBrO_3$. a : first peak; b: second peak.

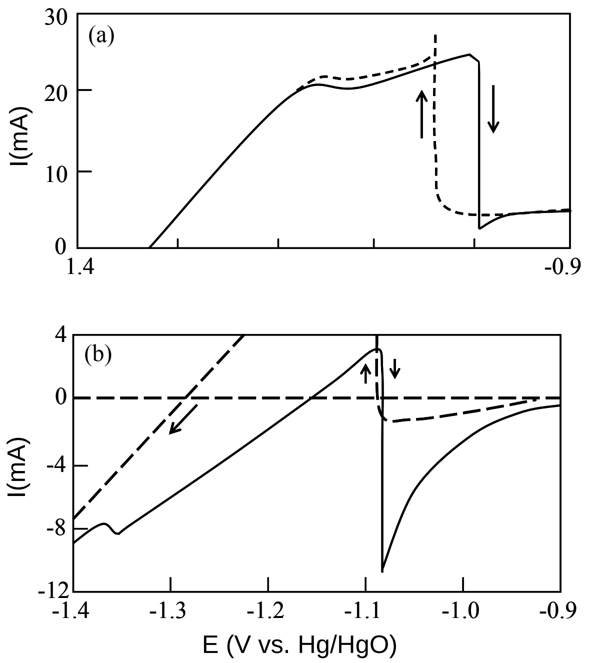

Fig. 2. Effect of the bromate concentration on the polarization behavior: RDE, 1200 rpm, 2 mV/s, 29°C, 1.0 M KOH (a) with 2 g/L $KBrO_3$; (b) with 16.7 g/L $KBrO_3$.

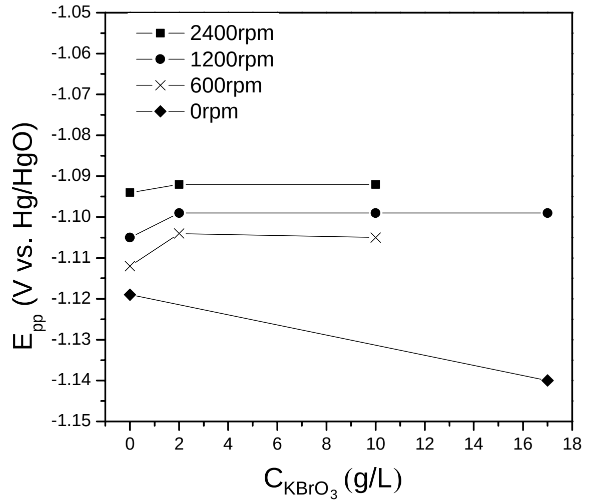

Fig. 3. Effects of the bromate concentration and hydrodynamics on the passivation potential on a RDE: 1.0 M KOH, 1200 rpm, 2 mV/s, 29°C.

measured in 1 M KOH solutions containing various concentrations of potassium bromate additives under controlled hydrodynamic conditions. Due to the addition of potassium bromate additives, the primary passive potential shifted to more positive values. As can be seen from Fig. 3, all the solutions with different potassium bromate contents (but under the same hydrodynamic conditions) had essentially the same primary passive potential, particularly in the high bromate concentration region. Electrodes operated under different hydrodynamic conditions showed the same trend over the entire concentration range studied. Figure 3 also shows that for solutions with identical compositions, the primary passive potential increased anodically with the increasing rotation rate. The observed relatively weak rotation rate dependence suggests that the type of electrode processes was not strongly mass transport controlled. These observations indicate that the addition of potassium bromate contributed a depassivating action for the zinc electrode in alkaline electrolytes in this convection-dominated system.

On stationary electrodes, mass transport limitations become more important and sweep rate experiments can yield information regarding the severity of these limitations. Figure 4 shows that the potentials at which the first and the second peaks appeared were essentially unaffected by the sweep rate but that the introduction into the alkaline solution of potassium bromate lowered the potential necessary for the onset of passivation. These experimental results show that potassium bromate has no beneficial effect for a zinc electrode in pure diffusion-controlled mode. The peak potentials observed here were virtually independent of the rate of change of the potential, indicating that the interfacial redox transition is a rapid process in the prepassive region.

In order to gain quantitative insight into the dissolution kinetics, a potentiostatic technique was employed to measure the steady state currents at different rotation rates for the first rising portion of the respective polarization curves. Typical plots of the logarithm of the current against potential are shown in Fig. 5. The data in this figure may be constructed approximately as two straight lines with different slopes. In other words, these experimental results show that the anodic Tafel slope is a function of the potential in the active dissolution region. Using lin-

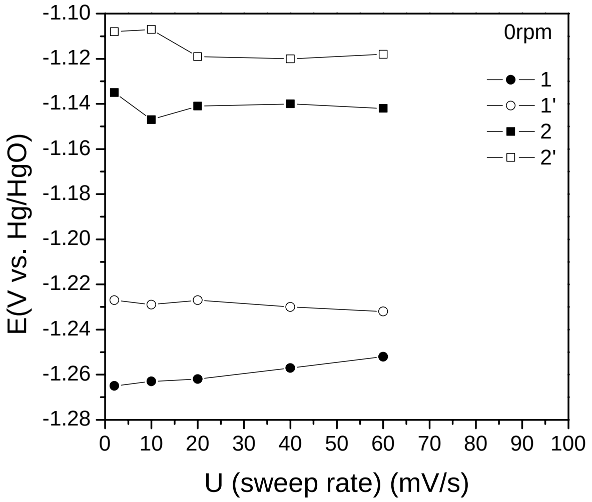

Fig. 4. Effect of the sweep rate on the polarization for a stationary RDE. 1 and 2 indicate, respectively, the first and second peaks in 1.0 M KOH + 0.1 M $KBrO_3$. 1′ and 2′ indicate, respectively, the first and second peaks in 1.0 M KOH.

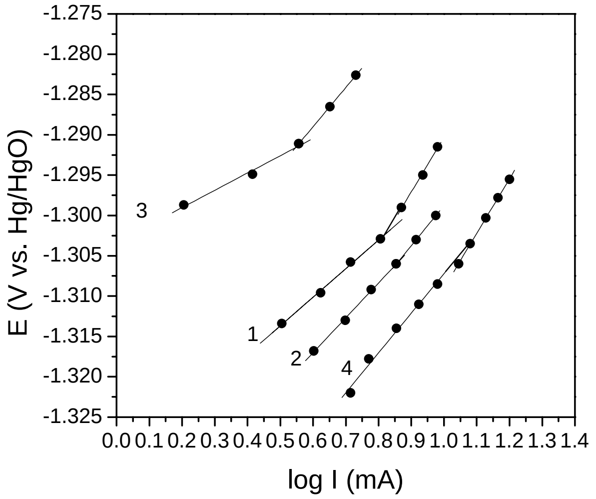

Fig. 5. Semilogarithmic plot of the current against potential as a function of the bromate concentration and rotation rate: 1.0 M KOH, 29°C. Curve 1: with 2 g/L $KBrO_3$, 600 rpm; curve 2: with 2 g/L $KBrO_3$, 2400 rpm; curve 3: with 10 g/L $KBrO_3$, 600 rpm; curve 4: without $KBrO_3$, 2400 rpm.

ear regression analysis, the Tafel slopes for the first section of curves 1-4 (I) were experimentally determined to be 35.4, 43.2, 23.5, and 50.6 mV/decade, respectively. The Tafel slopes were found to be 68, 49, 48, and 67 mV/decade for the second section of curves 1-4 (II), respectively. These results show that the anodic Tafel slope decreased with the introduction of potassium bromate (curves 2 and 4) and also decreased with the increasing potassium bromate concentration (curves 1 and 3). The nominal anodic Tafel slope also increased with the increasing rotation rate (curves 1 and 2), as shown in Fig. 5.

PROPOSED KINETIC MODEL

Based primarily on the observed phenomena and the data from the rotating disk electrode experiments, the following kinetic scheme is proposed. Firstly, the invariance of the shape of the polarization curves suggests that the basic reactions for the anodic dissolution of zinc in alkaline electrolyte solutions, with or without the introduction of potassium bromate, are essentially identical. In the initial dissolution region, the following reactions are considered to be of greatest importance (Prentice *et al.*, 1991):

$$Zn + OH^- = ZnOH_{ads} + e^-, \qquad (3)$$

$$ZnOH_{ads} + 2OH^- = Zn(OH)_3^- + e^- \quad \text{rds}, \qquad (4)$$

$$Zn(OH)_3^- + OH^- = Zn(OH)_4^{2-}, \qquad (5)$$

where rds indicates the rate-determining step, and the subscript ads denotes the species in the adsorbed state.

At more positive potentials, reaction (3) can provide $ZnOH_{ads}$, which enters into the following parallel reaction path (Chang and Prentice, 1989):

$$ZnOH_{ads} + OH^- = Zn(OH)_{2ads} + e^-, \qquad (6)$$

$$Zn(OH)_{2ads} + OH^- = Zn(OH)_3^- \quad \text{rds}, \qquad (7)$$

$$Zn(OH)_3^- + OH^- = Zn(OH)_4^{2-}. \qquad (8)$$

It has been demonstrated that the above reaction scheme (the reactions of Eqs. (3)-(8)) can simulate the general features of the experimental curves for pure potassium hydroxide solution cases (Chang and Prentice, 1989; Prentice *et al.*, 1991).

Secondly, the appearance of the first peak, which exhibits the cathodic current characteristic (Fig. 2(b)), suggests that a certain parallel reduction reaction occurs concurrently with the anodic dissolution of zinc. We assume that this reaction involves the reduction of bromate through the following steps:

$$BrO^-_{3\ (solution)} = BrO^-_{3\ ads}, \qquad (9)$$

$$BrO^-_{3\ ads} + 3\ H_2O + 6e^- = Br^-_{ads} + 6\ OH^- \ \text{rds}.(10)$$

The standard potential for the reaction of Eq. (10) is 0.50 $V_{Hg/HgO}$ in alkaline media, and the electrode process is highly irreversible with a very large overpotential (Heyrovsky and Kuta, 1966).

Since we have parallel paths, the overall rate referring to zinc dissolution is equal to the sum of the rates in the three parallel reaction sequences:

$$r = r_4 + r_7 - r_{10}. \qquad (11)$$

The expression for the corresponding total current density can, then, be derived using the Langmuir kinetics. Let the fractional surface coverage by the bromate ions, the monovalent zinc hydroxide, and the divalent zinc hydroxide be θ_1, θ_2, and θ_3, respectively; then, the fraction of the bare electrode is given by $1-\theta_1-\theta_2-\theta_3$. The result is the following total current density expression for the proposed model:

$$
\begin{aligned}
i = 2F\{&k_{f_4}\,\theta_2 C^{2}_{\mathrm{OH^-}}\exp(\beta_2 FE/RT) \\
&- k_{r_4}(1-\theta_1-\theta_2-\theta_3)\,C_z\exp[-(1-\beta_2)FE/RT]\} \\
&+ 2F(k_{f_7}\theta_3 C_{\mathrm{OH^-}} - k_{r_7}C_z) \\
&- 6Fk_{f_{10}}\theta_1\exp(-6\alpha_1 FE/RT), \qquad (12)
\end{aligned}
$$

where F is the Faraday constant, the k's are the kinetic rate constants, C_i is the interfacial concentration of species i, the α and β terms are the symmetry factors, R is the gas constant, T is the absolute temperature and E is the applied potential with respect to a given reference electrode. The subscripts f and r refer to the forward reaction and the reverse reaction, respectively, and the subscript z denotes $\mathrm{Zn(OH)_3^-}$.

In a kinetic scheme involving more than one step, it is generally assumed that the rate-determining steps control the overall reaction rate and that other steps are rapid and proceed essentially at equilibrium. Therefore, the fractional surface coverage can be expressed in terms of the equilibrium constants, K's, and other parameters for those reactions that can be treated as being at equilibrium. Then, from these relations, we can obtain explicit expressions for θ_1, θ_2, and θ_3, respectively. Substituting these expressions into Eq. (12) yields

$$
\begin{aligned}
i = [&-6Fk_{f_{10}}H_1\exp(-6\alpha_1 FE/RT) \\
&+ 2Fk_{f_4}H_2C^{2}_{\mathrm{OH^-}}\exp(\beta_2 FE/RT) \\
&+ 2Fk_{f_7}H_3C_{\mathrm{OH^-}}]/H, \qquad (13)
\end{aligned}
$$

where $H_1 = K_1C_1/(1 + K_1C_1)$, $H_2 = K_2\{1 - [K_1C_1/(1 + K_1C_1)]\}C_{\mathrm{OH^-}}\exp(FE/RT)$, $H_3 = K_2K_3\{1 - [K_1C_1/(1 + K_1C_1)]\}C_{\mathrm{OH}}^{2}\exp(2FE/RT)$, and $H = H_1 + H_2 + H_3$. Here, C_1 denotes the concentration of $\mathrm{BrO_3^-}$, $K_1 = k_{f_9}/k_{r_9}$, $K_2 = k_{f_3}/k_{r_3}$, and $K_3 = k_{f_6}/k_{r_6}$.

Equation (13) thus gives the overall reaction rate in terms of reacting species compositions and the parameters of the various steps. This expression is rather complicated for general case. In some limiting cases, it can be transformed into a simpler form. For instance, when $H_2 >> H_3$, we obtain the following equation:

$$
\begin{aligned}
i = [&-6Fk_{f_{10}}H_1\exp(-6\alpha_1 FE/RT) \\
&+ 2Fk_{f_4}H_2C^{2}_{\mathrm{OH^-}}\exp(\beta_2 FE/RT)]\,/\,\{H_1 + K_2\{1 \\
&- [K_1C_1/(1+K_1C_1)]\}C_{\mathrm{OH^-}}\exp(FE/RT)\}. \qquad (14)
\end{aligned}
$$

Thus, the reaction order with respect to bromate is a fractional number less than unity, depending on the potential applied. And the formal reaction order with respect to hydroxide is between 1 and 2. However, when $H_2 << H_3$, we get

$$
\begin{aligned}
i = [&-6Fk_{f_{10}}H_1\exp(-6\alpha_1 FE/RT) \\
&+ 2Fk_{f_7}H_3C_{OH^-}]/\{H_1 + K_2K_3\{1-[K_1C_1/ \\
&(1+K_1C_1)]\}\,C^{2}_{\mathrm{OH^-}}\exp(2FE/RT)\}. \qquad (15)
\end{aligned}
$$

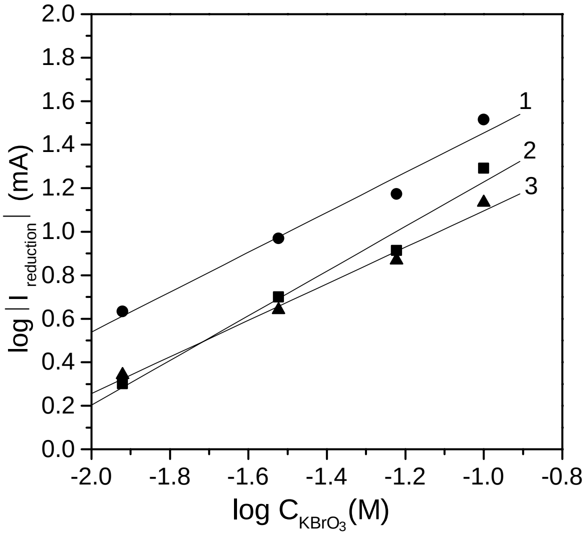

Fig. 6. Determination of the reaction order with respect to bromate at (1) the first peak, (2) the second peak, and (3) –1.28 V: RDE, 1200 rpm, 29°C, 1.0 M KOH.

This equation indicates that the order of the reaction with respect to hydroxide will lie between 1 and –1 but that the reaction order with respect to bromate will remain less than unity.

COMPARISON WITH EXPERIMENTAL DATA

The reaction orders at different potentials corresponding to the active dissolution and prepassive regions, respectively, have been determined. The proposed kinetic model considers the cathodic reduction of bromate and the anodic dissolution of zinc occurring along parallel paths. Thus, a decrease in the total current observed in the bromate-containing alkaline solutions during the anodic dissolution of zinc is mainly caused by the contribution of bromate reduction. As a first approximation, the reduction current of bromate is equal to the difference in the currents measured with and without the presence of bromate. Figure 6 plots the logarithm of the reduction current of bromate versus the logarithm of the bromate concentration at different applied potentials. The experimentally determined reaction orders for bromate are 0.84, 0.92, and 1.03 at –1.28 $V_{\mathrm{Hg/HgO}}$, the first peak, and the second peak, respectively. All values were determined using the linear regression method. The reaction orders vary with the potential and are essentially less than unity, as predicted by the proposed kinetic model. The agreement between the experimental results and the predictions provides support for the proposed reaction scheme.

At potentials well above the reversible potential for a rotating disk electrode in an electrolyte solution, the current is related to the relevant parameters in the following equation (Thirsk and Harrison, 1967):

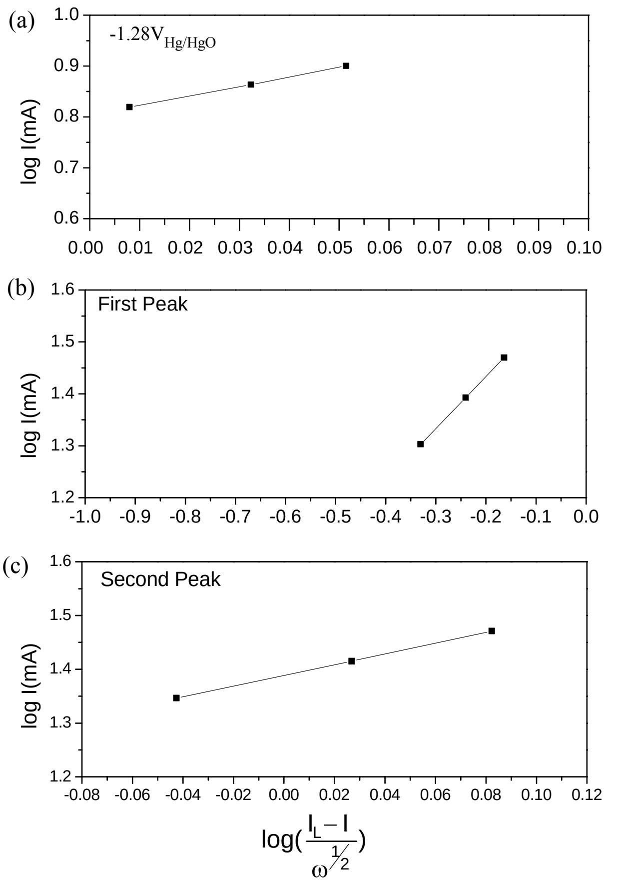

Fig. 7. Determination of the reaction order for hydroxide at 29°C at (a) –1.28 V, (b) the first peak, and (c) the second peak.

$$\log I = \log [(A^*)^{1-b} B^b k_s] + b \log [(I_L - I)/\omega^{1/2}], \tag{16}$$

where $A^*=nFS$, $B=1.61D^{-2/3}\nu^{1/6}$, S is the electrode area, I_L is the limiting current, ω is the rotation rate, D is the diffusion coefficient, ν is the kinematic viscosity, and b is the reaction order with respect to OH^-. For the present system, typical plots of log I versus log $[(I_L - I)/\omega^{1/2}]$ are presented in Fig. 7. The experimentally determined reaction orders for hydroxide are 1.86, 1.0, and 1.0 at –1.28 V (corresponding to the active dissolution region), the first peak (corresponding to the prepassive region), and the second peak (corresponding to the primary passive potential), respectively. Apparently, agreement is again obtained between the experimental results and the proposed kinetic model.

The semilogarithmic plot in Fig. 5 shows a slope of approximately 50 mV/decade for the rising part of the current-bias potential curve for the dissolution of zinc in a 1 M KOH solution (Fig. 5, curve 4). However, with the addition of potassium bromate, the slope becomes less than 50 mV/decade (Fig. 5, curve 2). Furthermore, the Tafel slope decreases with the increasing potassium bromate concentration (Fig. 5, curves 1 and 3). These observations are consistent with the model predictions, as demonstrated below.

Contributions to the total current density from individual reactions have been investigated previously for pure KOH solution cases (Prentice *et al.*, 1991). It was found that r_4 was much larger than r_7 for the rising portion of the polarization curve. The total current density can, then, be written as

$$\begin{aligned} i = 2F\{&k_{f_4}\theta_2 C^2_{OH^-} \exp(\beta_2 FE/RT) \\ &- k_{r_4}(1-\theta_1-\theta_2-\theta_3)\, C_z \exp[-(1-\beta_2)FE/RT]\} \\ &-6Fk_{f_{10}}\theta_1 \exp(-6\alpha_1 FE/RT). \end{aligned} \tag{17}$$

Based on this equation, we can make several predictions. The Tafel slopes are obtained directly from Eq. (17). The apparent anodic Tafel slope for the dissolution of zinc in an alkaline solution with the presence of bromate is

$$\begin{aligned} \partial E/\partial \log i = 2.3\{&-6Fk_{f_{10}}\, \theta_1 \exp(-6\alpha_1 FE/RT) + \\ &2Fk_{f_4}\, \theta_2 C^2_{OH^-} \exp(\beta_2 FE/RT) - 2Fk_{r_4}\,(1-\theta_1-\theta_2)C_z \\ &\exp[-(1-\beta_2)FE/RT]\}/\{[36Fk_{f_{10}}\theta_1\alpha_1 F/RT] \\ &\exp(-6\,\alpha_1 \mathrm{FE/RT}) + 2Fk_{f_4}\, \theta_2 C^2_{OH^-}\, \beta_2 F/RT] \\ &\exp(\beta_2 FE/RT) + [2Fk_{r_4}\,(1-\theta_1-\theta_2) \\ &C_z(1-\beta_2)F/RT] \exp[-(1-\beta_2)FE/RT]\}. \end{aligned} \tag{18}$$

This expression indicates that the anodic Tafel slope is a function of the species concentration, applied potential, and relevant parameters, and that it is not a constant. According to this expression, increasing the bromate concentration results in a decrease of the Tafel slope. Furthermore, increasing the rotation rate will increase the interfacial concentrations of the relevant species (Chang and Prentice, 1985), and this effect will cause the Tafel slope to increase. Equation (18) also shows that the first term in the denominator and in the numerator, respectively, can be dropped in the bromate-free case; then, the denominator becomes smaller while the numerator becomes larger. Therefore, the Tafel slope is largest in the pure KOH solution case. These predicted trends are all consistent with the experimental observations (Fig. 5). The exact Tafel slope for the corresponding pure KOH solution case can be shown to be

$$\partial E/\partial \log i = 2.3RT/[(2-\beta_2)F - H^*F/(1+H^*)], \tag{19}$$

where $H^* = k_{f_3} C_{OH^-}/k_{r_3} \exp(-FE/RT)$. Since H^* is a function of the potential, the Tafel slope also varies with the applied potential. Furthermore, it can be shown that $H^*/(1+H^*)$ is a monotonically increasing function varying from 0 to 1. Hence, at room temperature, depending on the applied potential, the Tafel slope may change from the lower limit (about 40 mV/decade) to the higher limit (about 120 mV/decade), if β_2 is selected as 0.5. A few additional points should be noted. Equation (19) shows that the so-called Tafel slope is a function of the concentration and potential, and is not constant. While the data in Fig. 5 may be constructed approximately as two straight lines with different slopes (as shown in the figure), a significantly better fit of the data is a single continuous curve with varying slopes.

CONCLUSION

The electrodissolution behavior of zinc in potassium hydroxide solutions containing bromate additives has been examined experimentally using the rotating disk electrode technique. In bromate-containing solutions, the zinc anodes passivated at slightly more anodic potentials. However, the apparent total current observed during the onset of passivation decreased with the increasing bromate content in the potassium hydroxide solution. Furthermore, the anodic Tafel slope became smaller with the addition of bromate and varied with the applied potential.

A kinetic model based on the Langmuir competitive chemisorption approach has been developed and tested. The model predictions are consistent with the observed trends for the anodic dissolution of zinc in potassium hydroxide electrolyte solutions containing bromate. It has been shown that the parallel reduction of bromate ions can cause a decrease in the Tafel slope. In addition, the potential dependence of the Tafel slope is due to the adsorption of the reacting species on the electrode surface. The agreement with the experimental data is encouraging. This model gives us physical insight into how the bromate dynamically interacts with the anodic dissolution reactions of zinc. However, further study is needed to establish the exact nature and structure of bromate on the zinc electrode surface.

ACKNOWLEDGEMENT

This research was supported by the National Science Council of the Republic of China under contract no. NSC 89-2214-E-032-015.

REFERENCES

Armstrong, R. D. and M. F. Bell, *Electrochemistry-Specialist Periodical Reports*, Vol. 4, p.1, The Chemical Society, London, U.K. (1971).

Aslam, M. and J. A. Harrison, "An Electrode Kinetic Investigation of the Zinc Deposition-Dissolution Reactions," *Surf. Technol.*, **12**, 3 (1981).

Binder, L. O., "Metallic Negatives," *Handbook of Battery Materials*, Part II, Section 6.3.7, J. O. Besenhard, Ed., Wiley-VCH, Weinheim, FRG (1999).

Bockris, J. O'M, Z. Nagy, and A. Damjanovic, "On the Deposition and Dissolution of Zinc in Alkaline Solutions," *J. Electrochem. Soc*., **119**, 285 (1972).

Cachet, C., U. Stroder, and R. Wiart, "Impedance Measurements During the Cycling of a Zinc Electrode," *J. Appl. Electrochem.*, **11**, 613(1981).

Chang, Y. C. and G. Prentice, "Anodic Dissolution of Zinc Electrodes in Alkaline Electrolyte: Mass Transport Effects," *J. Electrochem. Soc*., **132**, 375 (1985).

Chang, Y. C. and G. Prentice, "A Model for the Anodic Dissolution of the Zinc Electrode in the Prepassive Region," *J. Electrochem. Soc*., **136**, 3398 (1989).

Flerov, V. N., "The Influence of Certain Addition Agents on the Passivation of a Zinc Anode and on the Performance of Alkali-Zinc Cells," *J. Appl. Chem. USSR*, **31**, 1306 (1959).

Heyrovsky, J. and J. Kuta, *Principles of Polarography*, p. 242, Academic Press, New York, U.S.A. (1966).

Kawamura, G. and Y. Maki, "A Study of Insoluble Zinc Electrodes for Alkaline Secondary Batteries. I. Insolubilizing the Zincate Ion by Calcium Hydroxides," *Denki Kagaku*, **48**, 592 (1980).

Littauer, E. L. and J. F. Cooper, "Zinc/Air Batteries," *Handbook of Batteries & Fuel Cells*, Section 30.2, D. Linden, Ed., McGraw-Hill, Inc., New York, U.S.A. (1984).

Liu, M. B., G. M. Cook, and N. P. Yao, "Passivation of Zinc Anodes in KOH Electrolytes," *J. Electrochem. Soc*., **128**, 1663 (1981).

Marshall, A., N. A. Hampson, J. S. Drury, and J. P. G. Farr, "The Effect of Potassium Silicate on the Dissolution of Zinc in Alkali," *Surf. Technol.*, **5**, 149 (1977).

Morgan, P. C., N. A. Hampson, and D. J. Spiers, "The Passivation of Zinc in Alkali," *Surf. Technol*, **12**, 245 (1981).

Nanis, L. and W. Kesselman, "Engineering Applications of Current and Potential Distributions in Disk Electrode Systems," *J. Electrochem. Soc.*, **118**, 454 (1971).

Newman, J., "Resistance for Flow of Current to a Disk," *J. Electrochem. Soc.*, **113**, 501 (1966).

Pletcher, D. and F. C. Walsh, *Industrial Electrochemistry*, 2nd Ed., p. 583, Blackie Academic & Professional, London, U.K. (1993).

Popova, T. I., "Passivation of Zinc in Alkaline Solution," *Sov. Electrochem.*, **8**, 469 (1972).

Prentice, G., Y. C. Chang, and X. Shan, "A Model for the Passivation of the Zinc Electrode in Alkaline Electrolyte," *J. Electrochem. Soc*., **138**, 890 (1991).

Prostakov, M. E., A. I. Levin, and V. P. Kochergin, "Anodic

Behaviour of Zinc and Tin in Alkaline Electrolytes," *Russ. J. Phys. Chem.*, **35**, 202 (1961).

Sato, Y., H. Niki, and T. Takamura, "Effects of Carbonate on the Anodic Dissolution and the Passivation of Zinc Electrode in Concentrated Solutions of Potassium Hydroxide," *J. Electrochem. Soc.*, **118**, 1269 (1971).

Sharma, R. A., "Physico-Chemical Properties of Calcium Zincate," *J. Electrochem. Soc.*, **133**, 2215 (1986).

Sharma, R. A., "Kinetics of Calcium Zincate Formation," *J. Electrochem. Soc.*, **135**, 1875 (1988a).

Sharma, R. A., "Equilibrium Zn/ZnO Electrode potentials vs. HgO/Hg Electrode," *J. Electrochem. Soc.*, **135**, 1996 (1988b).

Thirsk, H. R. and J. A. Harrison, *A Guide to the Study of Electrode Kinetics*, p. 86, Academic Press, London, U.K. (1967).

Zhang, X. G., *Corrosion and Electrochemistry of Zinc*, Sec. 14.2, Plenum Press, New York, U.S.A. (1996).

(*Manuscript received Apr.,12, 2005, and accepted Nov., 2, 2005*)

鋅在含溴酸鹽的鹼性溶液中的電化學溶解動力特性

張裕祺
淡江大學化學工程與材料工程學系

林岱儀　林俊一
國立台灣科技大學化學工程學系

摘　要

本文利用旋轉圓盤電極法研究溴酸鹽對鋅在氫氧化鉀溶液中陽極溶解行為的影響。實測結果顯示總溶解電流隨溴酸鹽濃度的提高而減小，又鈍化電位則因溴酸鹽的添加而增大，但迅達一飽和值，而該值乃隨電極轉速而異。再者 Tafel 斜率會因溴酸鹽的添加而減小。本研究依實驗結果提出一動力模式以闡明陽極溶解程序，並加以驗證。實驗觀測和模式預測頗相符，此乃支持本研究所提溴酸鹽的還原和鋅在氫氧化鉀溶液中陽極溶解乃並行反應的假定。